ARTICLE NO. 79-1531R

J80-177

Karman Vortex Shedding and the Effect of Body Motion

20007
20009
20016

L. E. Ericsson*
Lockheed Missiles & Space Company, Inc., Sunnyvale, Calif.

The unsteady aerodynamic characteristics of a circular cylinder in incompressible crossflow have been studied to obtain a better understanding of the coupling between body motion and Karman vortex shedding. It is found that the coupling is taking place through the effect of body motion on the boundary-layer development between stagnation and flow separation points. Using a moving wall/wall jet analogy, the experimentally observed effects of lateral and longitudinal oscillations on the Karman vortex shedding at subcritical Reynolds numbers can be explained. This permits an assessment to be made of the potential for self-excited oscillations in the different flow regimes. Where experimental results are available, they agree with this assessment. Basic flow similarity indicates that the unsteady flow concepts developed for prediction of dynamic stall of airfoils could be modified and applied to predict the observed effects of body motion on the Karman vortex shedding as well as the measured cylinder response.

Nomenclature

a	= oscillation amplitude
c	= reference length, $c=d$
d	= diameter
d_{max}	= maximum cross-sectional width
d_{2D}	= sectional drag, coefficient $c_d=d_{2D}/(\rho_\infty U_\infty^2/2)c$
f	= frequency of oscillating body
f_v	= frequency of vortex shedding
f_{v0}	$=f_v$ for stationary flow conditions
h	= width of vortex wake
h_s	= initial wake width
l	= sectional lift, coefficient $c_l=l/(\rho_\infty U_\infty^2/2)c$
Re	= Reynolds number based on d_{max} and freestream conditions
S, S_v, S_{v0}	= Strouhal number $S=fd_{max}/U_\infty$, $S_v=f_v d_{max}/U_\infty$, $S_{v0}=f_{v0}d_{max}/U_\infty$
U	= horizontal velocity
δ	= roughness height
θ_s	= separation angle on circular cylinder
ρ	= air density
ν	= kinematic viscosity
ω	= angular rate

Subscripts

s	= separated flow
v	= vortex shedding from oscillating cylinder
$v0$	= vortex shedding from stationary cylinder
W	= wall
∞	= freestream conditions

Introduction

THE various facets of the flow around circular cylinders are described in the reviews by Morkovin,[1] Wille,[2] and Berger and Wille.[3] Von Kármán[4] showed mathematically that only one vortex wake geometry was stable, one in which the vortices were forming an asymmetric vortex wake in which the ratio between lateral and longitudinal spacing is 0.28. Thus the wake Strouhal number is

$$f_{v0}h/\bar{U}_v = 0.28 \tag{1}$$

The mean convection velocity determined by experiments is $\bar{U}_v/U_\infty = 0.75$ for subcritical flow.[5,6] In turbulent boundary layers, the measured convection speed[7] is $\bar{U}_v/U_\infty = 0.80$, which should apply also to large-scale vortices according to a recent review.[8] As Eq. (1) gives

$$S_{v0} = 0.28\frac{\bar{U}_v}{U_\infty}\Big/\frac{h}{d} \tag{2}$$

and $\bar{U}_v/U_\infty$ varies only 6.7% between subcritical and supercritical flow, one finds that any major change of the Strouhal frequency S_{v0} has to be accomplished by a change of the flow separation and the associated wake width h.

Discussion

It will be shown how the Karman vortex shedding from stationary and nonstationary cylinders is dominated by the flow conditions at the boundary-layer separation. For a circular cylinder, Eq. (2) can be written

$$S_{v0} = 0.28\frac{\bar{U}_v}{U_\infty}\Big/\frac{h}{h_s}\frac{h_s}{d} \tag{3}$$
$$h_s/d = \sin\theta_s$$

where θ_s is the peripheral angle between stagnation and separation lines and $h/h_s \approx 1$.

Effect of Reynolds Number

Reynolds number has a profound effect on the vortex wake at very low speeds $Re<400$, and in the critical range $10^5 < Re < 3.5\times10^5$. With $\bar{U}_v/U_\infty = 0.75$ (Refs. 5 and 6) and $h \approx d$ for a circular cylinder in subcritical flow, one obtains $S_{v0} \approx 0.21$, which for $Re > 10^3$ is in good agreement with Rosko's subcritical formula[9]

$$S_{v0} = 0.212[1-(12.7/Re)] \tag{4}$$

For supercritical flow, with $\theta_s = \sin^{-1}(0.8) = 127$ deg, which is in agreement with experiments,[10,11] Eq. (3) gives $(S_{v0})_{supercrit} = 0.28$. Roshko[12] measured $S_{v0} = 0.27$, and others[13] have measured $S_{v0} = 0.28$. Figure 1 shows these results, together with those obtained in various other ex-

Presented as Paper 79-1531 at the AIAA 12th Fluid and Plasma Dynamics Conference, Williamsburg, Va., July 23-25, 1979; submitted Aug. 13, 1979; revision received Feb. 5, 1980.

Index categories: Nonsteady Aerodynamics; Jets, Wakes, and Viscid-Inviscid Flow Interactions; Subsonic Flow.

*Senior Consulting Engineer. Associate Fellow AIAA.

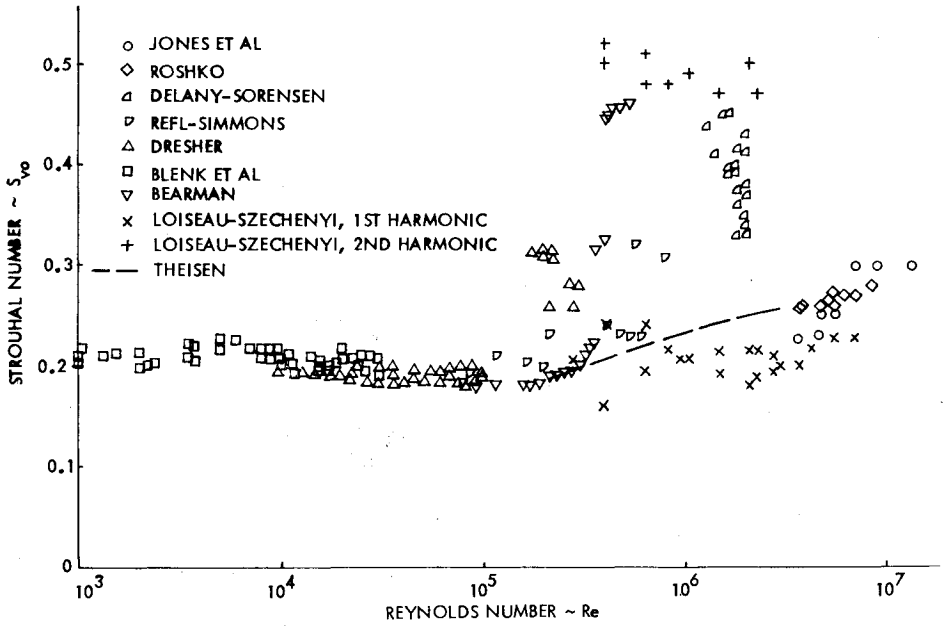

Fig. 1 Strouhal number as a function of Reynolds number.

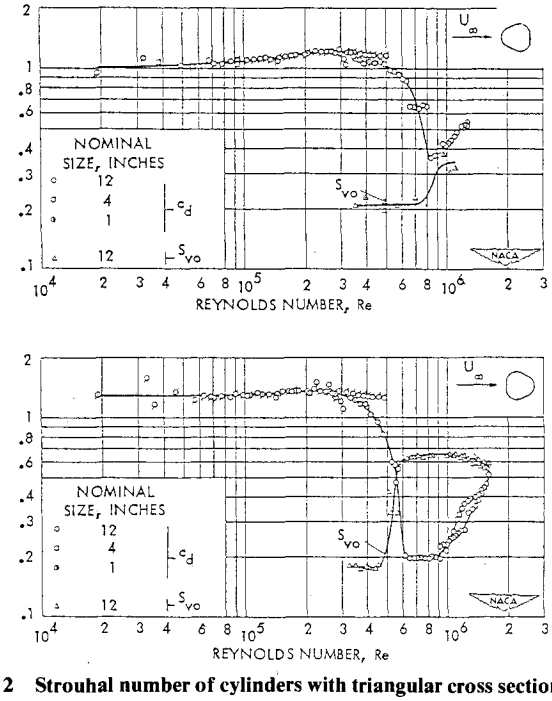

Fig. 2 Strouhal number of cylinders with triangular cross section.[14]

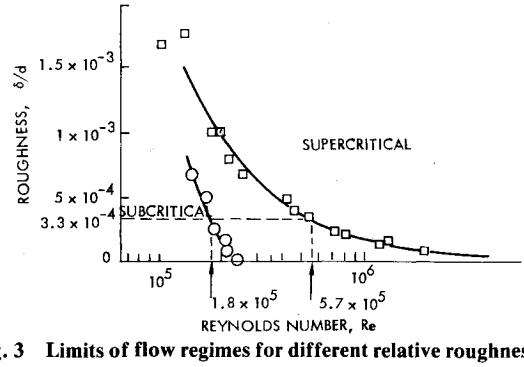

Fig. 3 Limits of flow regimes for different relative roughness.[25]

periments.[14-20] The various reasons for the large scatter of data in the critical Reynolds number region $10^5 < Re < 4 \times 10^6$ are discussed in Ref. 21. It can be seen that the "center frequency" computed by Theisen[22] provides a smooth transition from subcritical to supercritical Strouhal numbers $0.2 \times 10^6 < Re < 3.5 \times 10^6$.

While the Delany-Sorensen data[14] may not be quantitatively correct, they should, as the authors point out, give the correct qualitative effects of cross-sectional shape. Figure 2 shows an interesting comparison between two isoceles triangular cylinders, one with the apex forward, the other with the apex aft. In both cases, the maximum-exposed cross-sectional height is the same, and the Strouhal frequency at subcritical Reynolds number is, as a consequence, roughly the same. However, the Strouhal numbers measured at supercritical conditions are widely different. This is the result of widely different flow separation geometries. Assuming that the flow separates close to the flat base for the forward facing triangle, one obtains through the (h/d)-ratios discussed earlier, Eqs. (2) and (3), the ratio 1.4 between supercritical and subcritical Strouhal numbers, which compares rather well with the measured value. For the backward facing triangle, one would expect flow separation to occur at the start of the hemispherical base. This gives the ratio 3.6, which also is in good agreement with the experimental value.

Although Reynolds number is a very important parameter, it is not sufficient by itself to determine whether the flow on the cylinder is supercritical or subcritical. Surface roughness can change the effective critical Reynolds number by one order-of-magnitude[23] and wind-tunnel turbulence has a similarly large effect.[24] Figure 3 summarizes the effect of roughness on the Reynolds number boundaries of the critical region.[25] With the definition of "smooth" used by Schechenyi,[26] i.e., $(\delta/d)_{\text{smooth}} = 3.5 \times 10^{-5}$, Fig. 3 indicates that the critical region for a smooth cylinder extends from $Re < 2.5 \times 10^5$ to $Re > 2 \times 10^6$, the same Reynolds number range for which definite vortex periodicity is lacking (Fig. 1).

Criterion for Vortex Periodicity

Figure 3 illustrates how sensitive the transcritical Reynolds number boundaries are to roughness. Considering the spanwise variation of model roughness as well as wind-tunnel turbulence, one cannot, of course, expect the separated flow region to be truly two dimensional for critical Reynolds numbers. This conclusion is further supported by the results of Humphreys,[24] which show the boundary-layer transition process on a circular cylinder to be highly three-dimensional with a spanwise wave or cell pattern playing an important role.

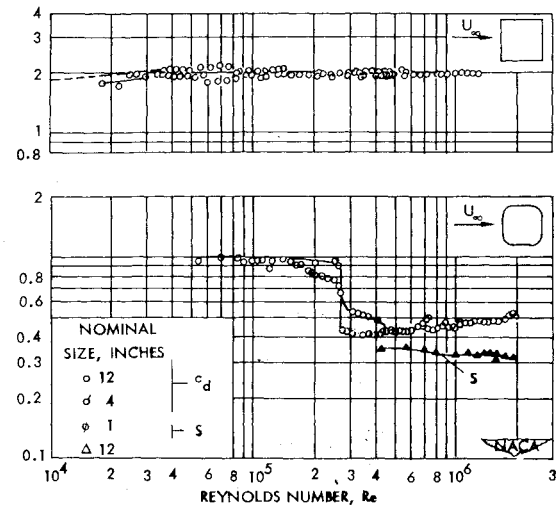

Fig. 4 Drag and Strouhal number for cylinder with square cross section.[14]

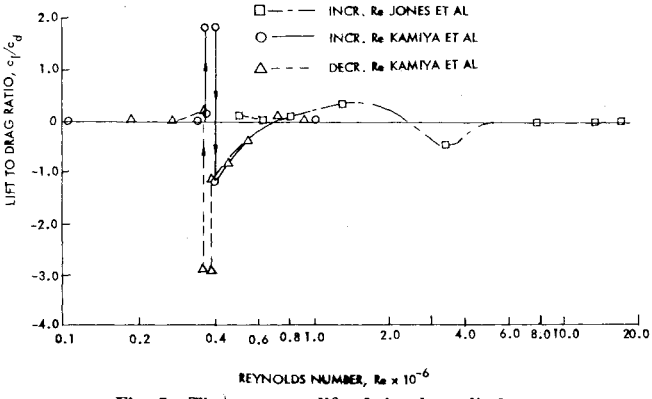

Fig. 5 Time-average lift of circular cylinder.

It appears, then, that the necessary condition for the establishment of vortex periodicity is the existence of a well-defined two-dimensional separated flow region over a certain spanwise extent[27] of four diameters or more, according to Theisen's results.[22] In that case, one should find no change in vortex periodicity when increasing the Reynolds number from 0.2×10^6 to 3.5×10^6 if the separation geometry remains unchanged. That this is indeed the case is illustrated by the results obtained by Delany and Sorensen[14] for a square cross section (Fig. 4). The drag of the sharp-edged model (top of Fig. 4) remains constant throughout the critical Reynolds number region indicating that the separation geometry remained unchanged. Hence one would also expect the shedding frequency to stay the same, according to the earlier discussion. For the rounded cross section in the bottom of Fig. 4, where the drag remained constant at its supercritical level for $0.4\times10^6<Re<2\times10^6$, the Strouhal number remained constant in accordance with the criterion postulated above. The results obtained for the time-average lift of a circular cylinder[18,28] also indicate that truly antisymmetric vortex shedding does not take place in the critical Reynolds number region $0.3\times10^6<Re<4.0\times10^6$ (Fig. 5).

Magnus Effects

The Magnus characteristics for rotating bodies in two-dimensional flow have recently been reviewed by Jacobson.[29] The classical positive lift is generated on a circular cylinder when the boundary layer remains laminar or turbulent. However, when boundary-layer transition occurs, large reversals of the Magnus effects are observed, resulting in the generation of negative lift.[30] A very thorough investigation of this phenomenon has been carried out by Swanson,[31] who also gives an historical account of the development of the concept of Magnus lift. Figure 6 shows the large effect on lift of small changes in rotational surface speed ratio ($U_W/U_\infty=\omega d/2U_\infty$). Figure 7 shows the static ($\omega=0$) cylinder drag variation through the critical Reynolds number range. The letters indicate where the various curves in Fig. 6 belong in Fig. 7.

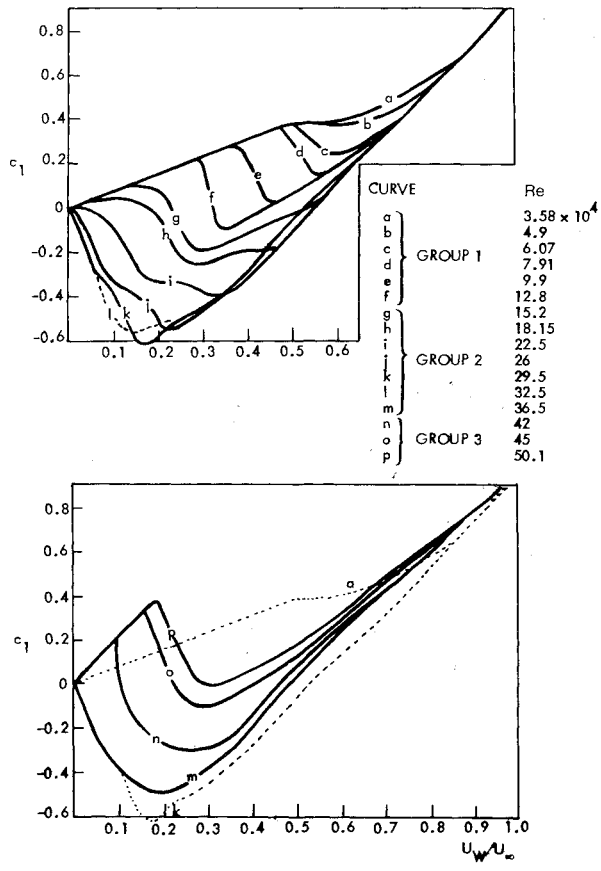

Fig. 6 Magnus lift of circular cylinder.[31]

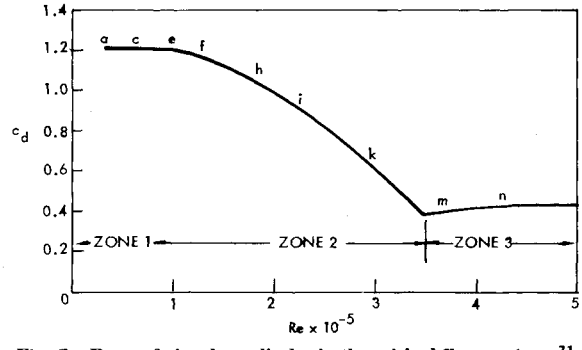

Fig. 7 Drag of circular cylinder in the critical flow regime.[31]

The moving wall effect is similar to that of a wall jet.[32] Thus, the downstream moving wall delays flow separation. For the upstream moving wall the effects are opposite and flow separation is promoted. Figure 8 shows the boundary-layer profiles computed by Swanson for $U_W/U_\infty=1$. Thus, in purely laminar or turbulent flow, positive lift is generated. However, in the critical Reynolds number range negative lift will be generated for the simple reason that the moving wall has the same effect on boundary-layer transition as on flow separation, delaying it on the downstream moving wall and promoting it on the upstream moving wall.

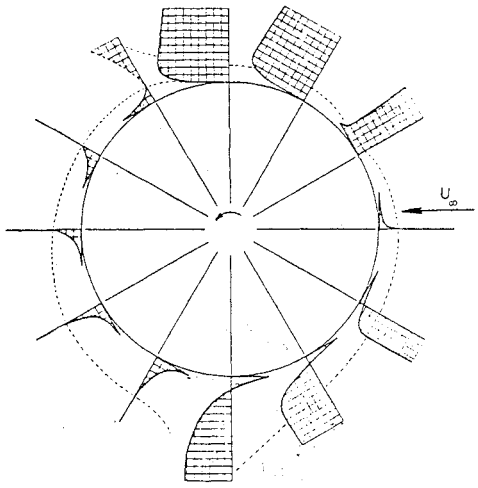

Fig. 8 Boundary-layer profiles at unit rotational speed ratio.[31]

Swanson[31] suggests that the reverse Magnus effect is qualitatively correlated by the relative Reynolds number $Re_{rel} = Re(1 + U_W/U_\infty)$. Examination of curve *l* in Fig. 6 and point *l* in Fig. 7 reveals the following: The full negative lift generation is accomplished with $U_W/U_\infty < 0.15$, whereas a change to the subcritical condition, which is generating the main portion of the negative lift (as illustrated by curve *m*), requires the Reynolds number to decrease from 3.3 to 1×10^5, a 60% change. The decrease in Reynolds number is $ReU_W/U_e \approx 1/2Re = 0.15/2$. That is, the direct Reynolds number effect is small. The wall jet effect of the moving wall accounts for 7/8 of the observed negative lift generation.

Keeping in mind that the adverse moving wall effects are stronger than the beneficial effects, the data trends in Fig. 6 can be explained. The fact that the moving wall effect on the lift for laminar† flow conditions is only one third of what it is for a turbulent† boundary layer, $\partial c_l/\partial(U_W/U_\infty) = 0.75$ for group 1 at $U_W/U_\infty < 0.5$ compared to $\partial c_l/\partial(U_W/U_\infty) = 2.2$ for group 3 at $U_W/U_\infty < 0.2$, reflects this dominance of the adverse effect. For supercritical flow conditions, group 3, the main effect is that of the upstream moving wall, causing a change from supercritical toward subcritical flow separation geometry. At the subcritical flow condition of group 1 data, the only effect of consequence is the downstream moving wall effect, causing a change from subcritical toward supercritical separation geometry. Thus the data in Fig. 6 show that it is three times as easy to weaken the boundary layer as it is to strengthen it.

In total agreement with this moving wall effect on the flow separation is the effect on transition displayed by the results in Fig. 6, as can be demonstrated by the use of Fig. 9. Consider first the group 1 data: When ω reaches the critical value, the adverse upstream moving wall effect causes boundary-layer transition upstream of the flow separation point, and the separation geometry changes rapidly from subcritical to supercritical. This effect completely overpowers the downstream moving wall effect on the laminar, subcritical separation on the top side. The result is an almost discontinuous loss of lift. When ω is increased sufficiently above the critical value, the top side also approaches supercritical flow conditions and the lift slope $\partial c_l/\partial(U_W/U_\infty)$ approaches the turbulent† level of group 3 data.

For the critical Reynolds numbers of the group 2 data, the main effect is probably that of the downstream moving wall. It delays transition more and more as ω is increased until transition disappears into the wake when ω reaches the critical value. As a result, the separation switches to subcritical on the top side, causing a large loss of lift. When the Reynolds number is at or near its critical value, curves *k*, *l*, and *m* in Fig. 6, this negative lift will be generated initially as soon as $\omega > 0$. Not until ω has been increased so that $U_W/U_\infty > 0.2$ is the condition reached which is sketched in the bottom of group 2 in Fig. 9. As ω is increased further, positive lift is generated at the turbulent rate (see Fig. 6).

Finally, for the supercritical Reynolds numbers of group 3, the turbulent level of lift is generated when ω is below the critical value. When the critical ω-value is reached, the downstream moving wall effect causes transition to move into the wake, as in the case of group 2 data (see Fig. 9). The resultant switch toward subcritical flow separation on the top side causes a more or less discontinuous loss of lift (see Fig. 6). Because of the higher Reynolds number and larger rotation rate with associated relatively stronger boundary layer, the full switch to laminar subcritical flow separation occurring for group 2 data is not realized. When ω is increased sufficiently above the critical value, the supercritical flow separation geometry sketched in Fig. 9 is reached and the turbulent lift slope $\partial c_l/\partial(U_W/U_\infty)$ is approached (Fig. 6).

It is evident from the preceding discussion that when ω is near its critical value, a very minute perturbation (through ω, U_∞, gusts, turbulence, etc.) will cause a dramatic change of the Magnus lift. The results obtained by Miller[33] show that this discontinuous jump can occur intermittently back and forth at the critical condition; in his case, $Re = 5 \times 10^5$ and $U_W/U_\infty = 0.27$.

Effect of Translatory Oscillation

Parkinson and Ferguson[34,35] showed that the Karman vortex street could be driven off its regular shedding frequency by oscillating the cylinder transversely to the flow at nearly resonant frequencies (Fig. 10). Stansby[36] recently showed that for large oscillation amplitudes this change in frequency could be as large as a 30% decrease or a 90% increase. Koopman[37] has shown that for very low Reynolds numbers there exists a threshold amplitude which must be exceeded before vortex "lock-in" occurs. Mei and Currie[38] report that Maekawa and Mizuno found in their test at high subcritical Reynolds numbers, $0.37 \times 10^5 < Re < 2.8 \times 10^5$, that the separation points on a stationary cylinder oscillated between 78 and 90 deg azimuth, while Landweber had found it to remain fixed when the cylinder described small amplitude translatory oscillations. However, in their own tests[38] at $Re = 1.67 \times 10^4$, they found the separation points to oscillate, in agreement with the findings by Schindel and Zartarian,[39] and the angular amplitude of the separation movement was approximately proportional to the relative translatory amplitude a/d.

That the coupling between the vortex shedding and the cylinder oscillation exists also at critical and supercritical flow conditions was demonstrated by Cincotta et al.[40] at the same meeting where Parkinson and Ferguson first showed their subcritical results.[34] At supercritical Reynolds numbers, the cylinder oscillation caused more than a threefold increase of the unsteady lift.[18]

The coupling between translatory oscillations and the vortex shedding for a circular cylinder has received a great deal of attention and has been extensively investigated both theoretically and experimentally. Jones et al.[18,40] found in their test at supercritical Reynolds numbers, $Re > 5.5 \times 10^6$, that the maximum response occurred at $f/f_{v0} = 0.99$ at a Strouhal number of $S = 0.28$. They also found that for this test condition the phase lag and associated negative damping (causing the large amplitude response) at $f/f_{v0} < 1$ changed to a phase lead and positive damping when f exceeded the natural vortex shedding frequency f_{v0}.

A question of great practical consequence is the possibility of obtaining vortex lock-in at higher harmonics, $f = 2f_{v0}$, $3f_{v0}$, etc. Stansby's results[36] at $Re \approx 10^4$ show that this can indeed occur (see Fig. 11). It is interesting to note that tertiary

†This "nomenclature" refers to the boundary-layer conditions at $\omega = 0$.

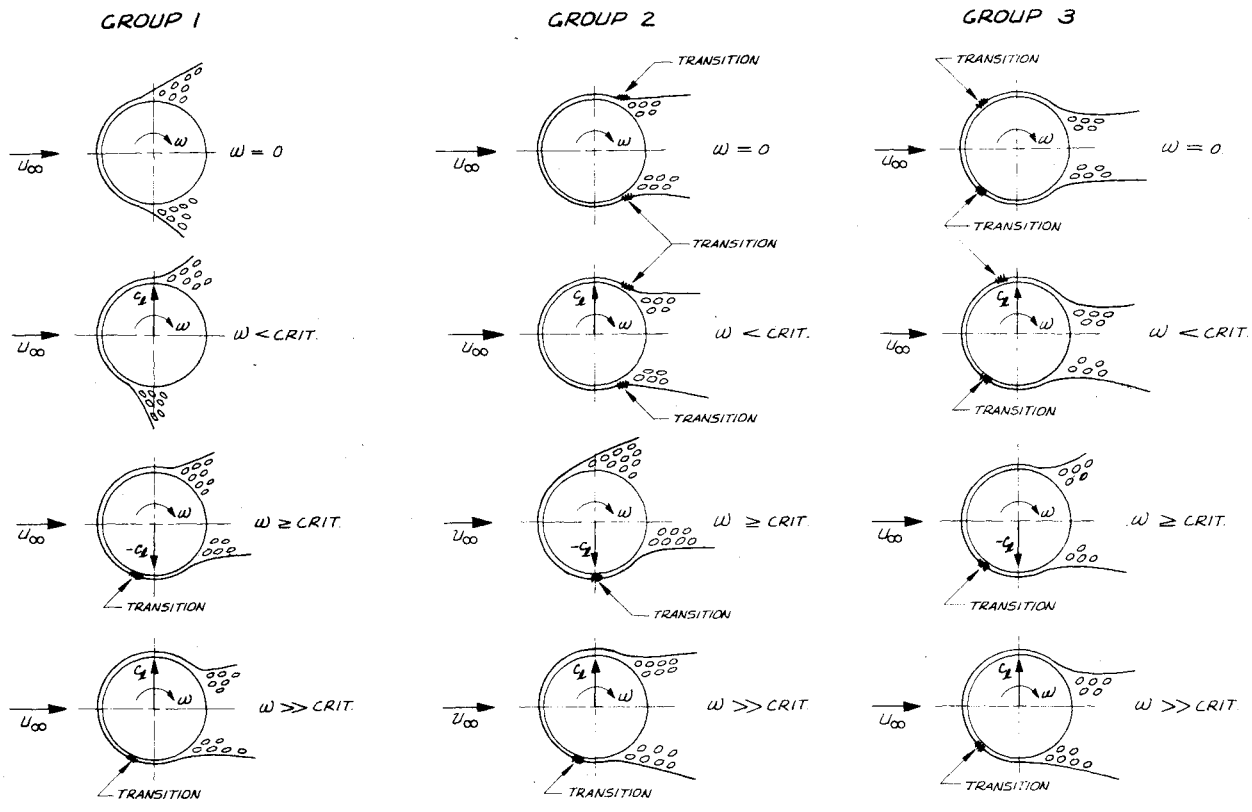

Fig. 9 Moving wall effects at subcritical, critical, and supercritical Reynolds number.

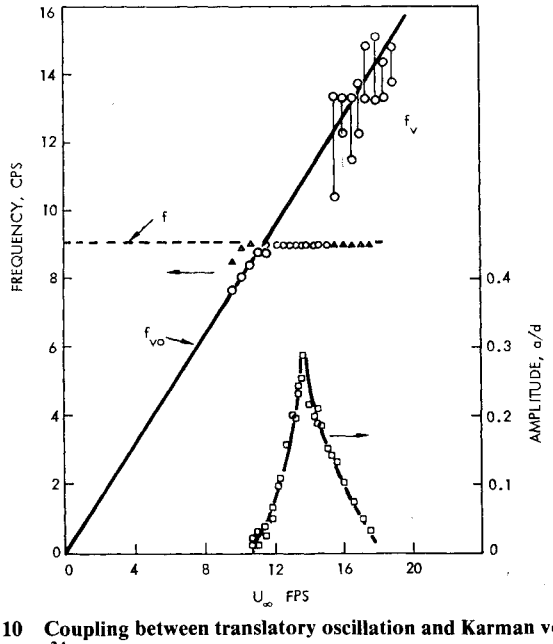

Fig. 10 Coupling between translatory oscillation and Karman vortex shedding.[34]

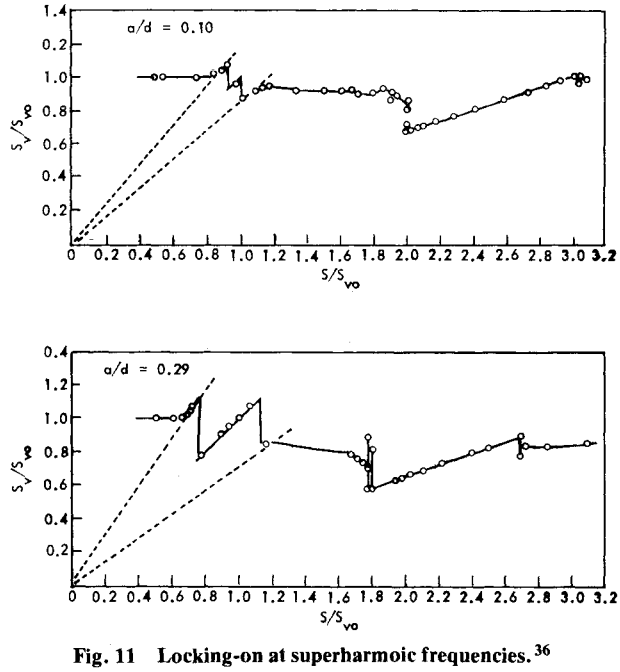

Fig. 11 Locking-on at superharmoic frequencies.[36]

locking-on is well documented, while secondary lock-in is definitely absent for the large amplitude oscillation ($a/d=0.29$). All experimental data show that lock-in occurs more readily the larger the oscillatory amplitude is. Consequently, the "wiggle" in the data for the lower amplitude ($a/d=0.10$) cannot have been a sign of tentative secondary lock-in, as was suggested by Stansby.

What can be the reason for this inefficiency of the even superharmonics in the lock-in phenomenon? Figure 12 illustrates one physical flow process that can explain this anomalous behavior, i.e., the moving wall effect discussed earlier in connection with Swanson's results[31] (Fig. 6). As was shown for the spinning cylinder, the adverse effect of the moving wall is the strongest, i.e., the effect of the upstream moving wall to promote separation. Thus, it is this effect that is illustrated in Fig. 12. The moving wall effect is caused by the transverse velocity component. It is, therefore, maximum at zero deflection, the case shown in Fig. 12, and is zero at maximum transverse deflection. The transverse velocity component is indicated by a solid velocity vector, and the vortex-induced lift is shown by an open force vector.

Figure 12 shows that when the forcing frequency is equal to or three times as large as the vortex shedding frequency for a stationary cylinder, the moving wall effect will adversely

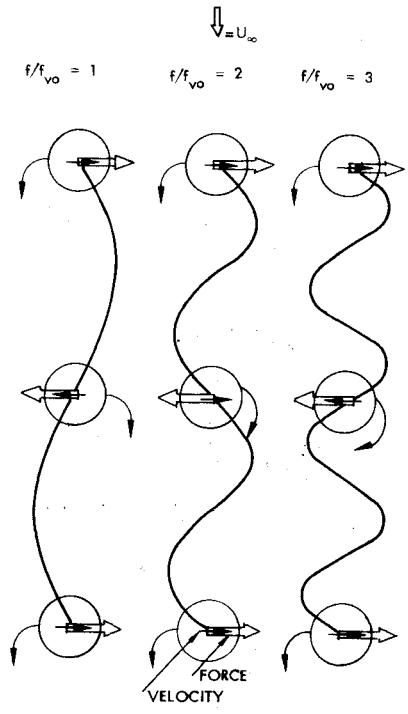

Fig. 12 Translatory moving wall effect on vortex shedding.

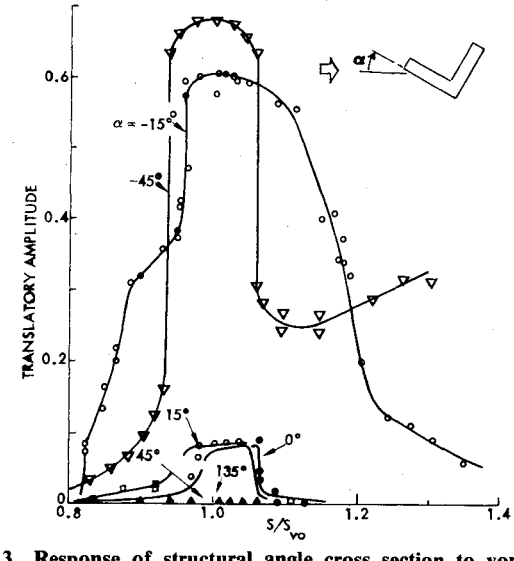

Fig. 13 Response of structural angle cross section to vortex excitation.[45]

affect the boundary layer approaching separation, thus promoting separation and thereby amplifying the generated transverse force, the lift. This occurs each time the transverse velocity reaches its maximum at the time of the vortex shedding event. In contrast, for the case that the driving frequency is twice the vortex shedding frequency, the moving wall effect promotes, respectively, opposes every other vortex shedding event, causing the net effect to be small‡ thus explaining the absence of lock-in for the even superharmonics (2nd, 4th, etc.). The force vector in Fig. 12 shows that the self-excited oscillations could occur for odd (but not even) harmonics.

The present state of the art in predicting the response of structures to vortex wakes has recently been described by

‡Stansby's spectral data[36] showed very broad harmonic peaks for $f=2f_{v0}$ both at $a/d=0.10$ and $a/d=0.29$, whereas the harmonic spikes are extremely narrow for $f=f_{v0}$ and $f=3f_{v0}$.

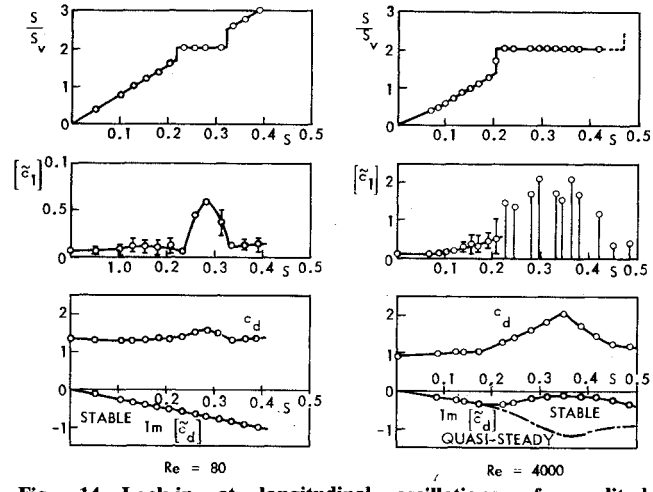

Fig. 14 Lock-in at longitudinal oscillations of amplitude $a/d=0.14$.[47]

Landl.[41] His experimental results show discontinuous amplitude increases and frequency hysteresis effects. He also found that the response could be double-valued in some instances, where the upper branch cannot be reached through self-excited oscillations but only after receiving an external disturbance that is larger than that corresponding to the lower amplitude level. This jump in response has also been measured by others.[42] Similar double-valued response characteristics have been observed also in three-dimensional separated flow.[43]

In regard to the theoretical treatments, they usually concentrate on solving the nonlinear mathematics needed to reproduce some of the experimentally observed response characteristics. Although some success has been obtained through this approach,[41] in most cases the agreement with experiment is poor, especially in regard to the response of the circular cylinder, the case studied by most researchers. This conclusion is also reached by Sarpkaya[44] in his critical review.§ All theories more or less disregard the flow separation process generating the wake. Common sense says that there is a large difference between the wake-body coupling mechanism for a flat-based wedge or plate, where the separation point is fixed by the geometry, and that for a cylinder, where the separation point is free to move. The experimental results obtained by Modi and Slater[45] (Fig. 13) for a structural angle section indicate that this separation point movement is a very important mechanism. Thus, the largest response was obtained when the angle was oriented with its concave section forward, in which case the separation point was free to move on the aft "boattail." In contrast, no significant response was seen for the opposite orientation, when the cavity was facing downstream and the separation points were fixed. Marris[46] has pointed out the importance of the moving separation point and suggests that the cylinder performing translatory oscillations could possibly be analyzed by applying Swanson's Magnus theory[31] to oscillatory rotation.

So far only transverse oscillations have been discussed. That the vortex lock-in occurs also for longitudinal, streamwise oscillations of a circular cylinder has been demonstrated in recent experiments[47] (Fig. 14). One notes with some surprise that first lock-in for longitudinal oscillations occurs at twice the natural Strouhal frequency. It is again the phasing of the moving wall effect[31] (Fig. 6) that

§Reference 44, which was published after the completion of the study[21] on which the present paper is based, is, in this author's opinion, the best review available of our current understanding of the Karman vortex shedding from stationary and nonstationary cylinders, which is restricted largely to subcritical flow.

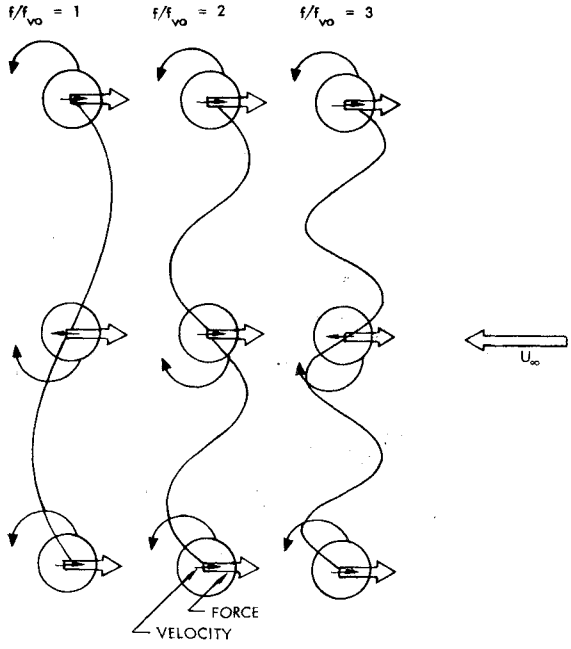

Fig. 15 Longitudinal moving wall effect on vortex shedding.

determines at what harmonic lock-in will occur (see Fig. 15). When the driving frequency is equal to or three times as large as the vortex shedding frequency for a stationary cylinder, the (maximum) moving wall effect (at zero deflection) will alternatingly promote and oppose the vortex shedding event, resulting in a net effect that is small. In contrast, when the driving frequency is twice (4, 6, etc., times) as large as the vortex shedding frequency, the moving wall effect will promote all the vortex shedding events, and the net effect is very powerful. At the higher Reynolds number, $Re = 4000$ in Fig. 14, the natural shedding frequency can be increased more than 100% with a longitudinal amplitude that is 14% of the cylinder diameter.

When the undamping force component generated by the motion-induced changes of the flow geometry (this is the only force component shown in Figs. 12 and 15) exceeds the damping force generated by the attached flow region on the cylinder, self-excited¶ oscillations will result, if not external (mechanical or structural) damping is supplied. Swanson's experiment with the rotating cylinder[31] will be used to assess the effect of Reynolds number on lateral and longitudinal oscillations. Figures 6 and 9 show, as discussed earlier, that at subcritical and supercritical Reynolds numbers positive Magnus lift was generated (group 1 and group 3 data, respectively), which in Fig. 12 translates to an undamping lateral force, with the potential for self-excited oscillations being greatest in the supercritical flow region. (The Magnus lift is 3 times larger there than for subcritical flow conditions.) At critical Reynolds numbers, however, negative Magnus lift was generated, which in Fig. 12 translates to a damping force. Thus one would not expect self-excited lateral oscillations to occur in the critical Reynolds number region. The measured drag (Fig. 16) shows that as the separation point moves from the subcritical to the supercritical position on the bottom side (Fig. 9), the drag decreases greatly, corresponding to an increased driving force in Fig. 15. The potential for this drag decrease and associated possibility of self-excited oscillations will increase with increasing subcritical Reynolds number. In

¶The term "self-excited," used here in conjunction with the Karman vortex shedding, is somewhat of a misnomer, as has been pointed out by Sarpkaya.[44] It is used here to designate the change from the usually benign body response to the wake-generated forcing function for positive net damping to the excessive, often catastrophic response resulting for negative damping.

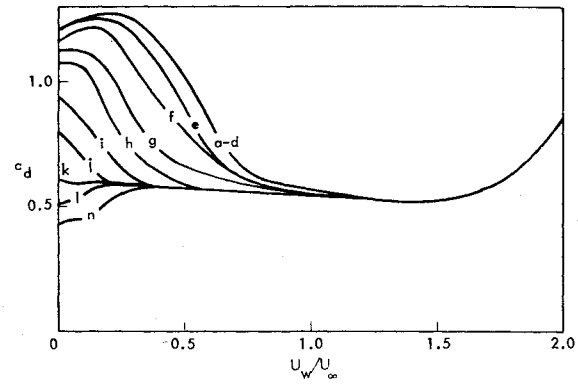

Fig. 16 Cylinder drag as a function of rotational speed ratio.[31]

the critical flow region, the potential for negative aerodynamic damping will exist, but the absence of pure harmonic vortex shedding at these Reynolds numbers makes it difficult to assess the potential for self-excited longitudinal oscillations. Finally, at supercritical flow conditions the critical moving wall effect is a change from turbulent supercritical to laminar supercritical flow conditions, producing a drag increase, which in Fig. 15 translates into a damping force. Thus, no self-excited longitudinal oscillations should occur at supercritical Reynolds numbers.

Based on the arguments just presented, one should find the following Reynolds number trends for a circular cylinder. At subcritical Reynolds numbers both translatory and longitudinal self-excited oscillations will occur with a probability and magnitude that increase with increasing Reynolds number, especially in the case of longitudinal oscillations. In the critical Reynolds number region no lateral self-excited oscillations are expected. The potential for longitudinal oscillations is somewhat uncertain. On the one hand, the undamping force initiating self-excited oscillations is present. On the other hand, true Karman vortex shedding is difficult to establish in the critical Reynolds number region due to the three-dimensional character of boundary-layer transition. It is, of course, possible that oscillations started by the presence of aerodynamic undamping will organize harmonic vortex shedding. No experimental data that could shed light on this situation were uncovered in the study[48] on which this paper is based. Finally, at supercritical Reynolds numbers, no longitudinal self-excited oscillations are to be expected; whereas the potential for lateral self-excited oscillations is greatest in this flow regime.

The next question is, of course, "Are these oscillation forecasts supported by experimental results?" Based on the data uncovered in the study,[48] the answer is a definite "yes." Translatory self-excited oscillations have been shown to exist both at subcritical[44] and supercritical[18] conditions; whereas to the best of the present author's knowledge no such results have been reported for the critical Reynolds number region. In regard to the potential for self-excited longitudinal oscillations, the results in Fig. 14 are in complete agreement with the present "forecast," showing the damping to decrease dramatically when the Reynolds number was increased from $Re = 80$ to $Re = 4000$. The existence of self-excited oscillations at higher Reynolds number is strongly indicated, as the potential would increase greatly acccording to the earlier discussion of the results in Fig. 16. No experimental results were found in the study[48] for critical or supercritical Reynolds numbers.

Reviewing Fig. 14 one can see that the longitudinal oscillation generates large lifting forces. This coupling between longitudinal and lateral degrees of freedom is of great practical interest. Based on the discussion of Figs. 11-16, the designer would be wise to avoid frequency ratios between lateral and longitudinal degrees of freedom that are multiples of 2.

Whether or not lock-in will also occur if the relative velocity change is obtained through harmonic perturbation of the freestream velocity $U(t) = U_\infty [1 + (\Delta U/U_\infty)\sin(2\Pi ft)]$ is not clear. The results obtained by Hatfield and Morkovin[49] appeared at the time to answer this question negatively. One point brought up when the data were presented was the possibility that the amplitude $\Delta U/U_\infty \approx 0.08$ was below an existing threshold value for excitation (see Refs. 37, 38, and 41). Morkovin was convinced, however, that the used 8% amplitude was high enough as it is 3-5 times larger than the velocity amplitude corresponding to the pressure fluctuations observed on a stationary cylinder. Figure 14 tends to support Morkovin's conclusion, i.e., the reason for the absence of lock-in was not lack of amplitude, but may have been a lack of frequency. The highest frequency used in the test[49] was 60% above the Strouhal frequency, which Fig. 14 indicates is not high enough for lock-in. It does not follow immediately from the data in Fig. 14 that locking-on will occur, as the wall-jetlike effect of the moving wall is absent in the case of oscillating freestream velocity. However, it is very likely as one has instead the effect of accelerating and declerating flow. (It should be emphasized that this discussion is limited to small amplitude oscillations, $\Delta U/U_\infty < 0.1$.) Reference 32 discusses how the accelerated flow and moving wall effects have similar influence on the flow separation. A definitive answer to the question of locking-on in the case of oscillatory perturbations of the freestream velocity cannot be obtained until the Hatfield-Morkovin experiment has been extended to higher frequencies. If the frequency of this horizontal velocity perturbation is far below the vortex shedding frequency, the vortex periodicity will adjust instantly (or nearly so) to the changed freestream conditions.[50]

This quasisteady behavior[50] is, however, not typical for subharmonic frequencies in general. The results reported in Ref. 51 show that coupling, leading to self-excited translatory oscillations of a cylinder, occurred when the cylinder natural frequency was one-third the regular vortex shedding frequency, but not when the fraction was one-half. Figure 17 shows the reason for this behavior. Again it is a question of the phasing of the moving wall effects. At $f=f_{v0}/2$ the translatory velocity-moving wall effect is zero for every other vortex shedding event taking place at maximum deflection. And at zero deflection, where the moving wall effect is maximum, it alternatively enhances and opposes the vortex shedding. Thus, no significant coupling can occur at this frequency. For $f=f_{v0}/3$, on the other hand, the maximum moving wall effect at zero deflection always enhances the vortex shedding, as in the case $f=f_{v0}$. For the intermediate pair of vortex shedding events, the translatory velocity and associated moving wall effects are very small and are of opposite signs, i.e., enhancing one and opposing the other of the two vortex shedding events. Thus the moving wall effect is negligible for these two intermediate shedding events at near-maximum deflection, and the dominant effect is the enhancement existing at zero deflection. Consequently, coupling occurs between translatory cylinder oscillation and vortex shedding for $f=f_{v0}/3$, although it is not as strong as for $f=f_{v0}$. Comparing Figs. 15 and 17 one concludes that subharmonic response at $f=f_{v0}/2$ should occur for longitudinal oscillations.

Future Analysis

It is clear that when the flow separation is not fixed by the geometry but is free to move, this degree of freedom has to be included in any realistic unsteady aerodynamic analysis. To do this using numerical methods is presently beyond our means.[44] The situation is very similar to that existing for the analysis of unsteady airfoil stall.[52,53] Thus a combined theoretical-experimental approach is needed similar to the one that has been used in the case of dynamic stall.[32,54] The time-space equivalence principle, now used to predict asymmetric vortex-induced loads on inclined bodies of revolution,[54] could

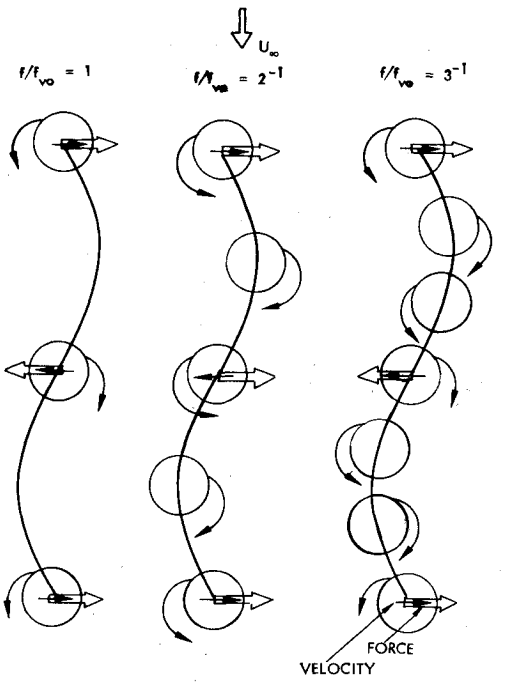

Fig. 17 Subharmonic translatory moving wall effects.

be applied in the reverse. Such application of the space-time equivalence between the leading-edge vortex on a delta wing and the "spilled" leading-edge vortex on a stalling airfoil proved very successful for the prediction of dynamic stall at high frequency and large amplitude.[55,56]

A first step toward a more realistic analysis of subcritical unsteady separation without recourse to the full Navier-Stokes equations has been taken by Sarpkaya et al.[44,57] The next step is to include the moving wall effect. This could, in theory, be accomplished for subcritical flow through numerical analysis in future large-scale digital computers.[58] However, at critical and supercritical flow conditions, where it is the coupling between body motion and boundary-layer transition that is the dominant flow mechanism, no such solution through numerical analysis is possible at present. A similar difficulty exists experimentally where simulation of the full-scale Reynolds number is needed in a dynamic test.[59] Such experimental simulation capability is presently becoming available, but the numerical simulation capability is not in sight.

Conclusions

Review and analysis of existing experimental results for a circular cylinder in incompressible crossflow reveals the following:

1) The vortex shedding frequency for a stationary, circular cylinder is defined by a Strouhal number that is close to 0.20 for subcritical flow $10^3 < Re < 2\times10^5$, and approximately 0.28 for supercritical flow $Re > 3.5\times10^6$. In the critical Reynolds number range, $2\times10^5 < Re < 3.5\times10^6$, the wake is random in character and the various measured discrete frequencies are caused by peculiar test conditions and measurement techniques.

2) The likely cause of the lack of well-defined periodicity in the critical Reynolds number region $0.2\times10^6 < Re < 3.5\times10^6$ is a lack of two-dimensionality in the separated-flow region.

3) Using von Kármán's stability criterion, the observed changes in shedding frequency can be predicted from the expected changes in flow separation geometry.

4) The vortex shedding process can be driven off its Strouhal frequency by translatory oscillations at near-resonant frequencies, the effect being highly dependent upon the translatory amplitude.

5) Longitudinal oscillations can also drive the vortex shedding off its basic frequency. However, in this case "lock-in" does not occur at near-resonant frequencies but when the forcing frequency first exceeds the second harmonic, $f > 2f_{v0}$.

6) Translatory oscillations at frequencies near the odd number super- and subharmonics of the resonant frequency will also appreciably influence the vortex shedding. Similar strong coupling is also to be expected for longitudinal oscillations at even number super- and subharmonics.

7) Based upon available experimental results, the designer should be aware that strong coupling effects are possible when the frequency ratios between lateral and longitudinal degrees of freedom are multiples of 2 or 0.5.

8) The selectivity of the locking-on process in regard to super- and subharmonics for translatory and longitudinal oscillations can be explained by the wall-jetlike effect of the moving wall discussed in detail for the spinning cylinder.

9) Exploring the wall-jetlike effect further indicates that self-excited oscillations of a circular cylinder can be expected for lateral oscillations at subcritical and supercritical flow conditions and for longitudinal oscillations at high subcritical Reynolds numbers. Available experimental data agree with this "wall-jet" prognosis.

10) Future analytic progress hinges strongly on efficient interactive use of theoretical and experimental methods.

Acknowledgment

The paper is based upon results obtained in a study for The Naval Surface Weapons Center, Silver Spring, Maryland, Contract N60921-77C-0234, under the direction of L. H. Schindel.

References

[1] Morkovin, M. V., "Flow Around a Circular Cylinder—A Kaleidoscope of Challenging Fluid Phenomena," ASME Symposium on Fully Separated Flows, edited by A. G. Hansen, May 1954, pp. 102-118.

[2] Willie, R., "On Unsteady Flows and Transient Motions," *Progress in Aerospace Science*, edited by D. Küchemann, Pergamon Press, London, Vol. 7, 1966, pp. 195-207.

[3] Berger, E. and Willie, R., "Periodic Flow Phenomena," *Annual Review of Fluid Mechanics*, Vol. 14, 1972, pp. 313-340.

[4] Von Kármán, Th. and Rubach, H., "Über den Mechanismus des Flüssigkeits und Luftwiderstands," *Physik. Zeitschrift*, Vol. 13, 1912, pp. 49-59.

[5] Young, J. O. and Hall, J. W., "Effects of Cavitation on Periodic Wakes Behind Symmetric Wedges," *Journal of Basic Engineering*, Vol. 88, March 1966, pp. 163-176.

[6] Dosanjh, D. S. and Asher, J. A., "Experimental Investigation of the Formation and Flow Characteristics of an Impulsively Started Vortex Sheet," *Journal of Basic Engineering*, Vol. 90, Dec. 1968, pp. 596-606.

[7] Kistler, A. L. and Chen, W. S., "The Fluctuating Pressure Field in a Supersonic Turbulent Boundary Layer," TR 32-277, Jet Propulsion Lab., California Institute of Technology, Pasadena, Calif., Aug. 1962.

[8] Roshko, A., "Structure of Turbulent Shear Flows: A New Look," 1976 Dryden Research Lecture, *AIAA Journal*, Vol. 14, Oct. 1976, pp. 1349-1357.

[9] Roshko, A., "On the Development of Turbulent Wakes from Vortex Sheets," NACA Rept. 1191, 1954.

[10] Achenbach, E., "Distribution of Local Pressure and Skin Friction Around a Circular Cylinder in Crossflow up to $Re = 5 \times 10^6$," *Journal of Fluid Mechanics*, Vol. 34, Pt. 4, 1968, pp. 625-639.

[11] Van Nunen, J.W.G., Persoon, A. J., and Tijdeman, H., "Analysis of Steady and Unsteady Pressure and Force Measurements on a Circular Cylinder at Reynolds Numbers up to 7.7×10^6," NLR, Netherlands, NLR TR 69102, May 1971.

[12] Roshko, A., "Experiments on the Flow Past a Circular Cylinder at Very High Reynolds Numbers," *Journal of Fluid Mechanics*, Vol. 10, 1960, pp. 345-356.

[13] Szechenyi, E. and Loiseau, H., "Portances Instationnaires sur un Cylindre Vibrant dans un Ecoulement Supercritique," *La Recherche Aérospatiale*, Jan.-Feb. 1975, pp. 45-57.

[14] Delany, N. K. and Sorensen, N. E., "Low-Speed Drag of Cylinders of Various Shapes," NACA TN-3038, Nov. 1953.

[15] Relf, E. F. and Simmons, L.G.F., "The Frequency Generated by the Motion of Circular Cylinders Through a Fluid," Aeronautical Research Council, Great Britain, ARC R&M No. 917, 1924.

[16] Drescher, H., "Messung der auf querangeströmte Zylinder ausgeübten zeitlich veränderten Drücker," *Zeitschrift fuer Flugwissenschaften*, Vol. 14, Helft 112, 1956, pp. 17-21.

[17] Loiseau, H. and Szechenui, E., "Analyse Experimentale des Portances sur un Cylindere Immobile Soumis a un Ecoulement Perpendiculaire a son Axe a des Nombres de Reynolds Elevés," *La Recherche Aérospatiale*, Sept.-Oct. 1972, pp. 279-291.

[18] Jones, Jr., G. W., Cincotta, J. C., and Walker, R. W., "Aerodynamic Forces on a Stationary and Oscillating Circular Cylinder at High Reynolds Numbers," NASA TR R-300, Feb. 1969.

[19] Blenk, H. F., Fuchs, D., and Liebers, F., "Über Messungen von Wirbelfrequenzen," *Luftfahrtforschung*, 12, 1935, pp. 38-41.

[20] Bearman, P. W., "On Vortex Shedding from a Circular Cylinder in the Critical Reynolds Number Regime," *Journal of Fluid Mechanics*, Vol. 37, Pt. 3, 1969, pp. 577-585.

[21] Ericsson, L. E., "Steady and Unsteady Vortex-Induced Asymmetric Loads, Review and Further Analysis," AIAA Paper 79-1531, Williamsburg, Va., July 1979.

[22] Theisen, J. G., "Vortex Periodicity in Wakes," AIAA Paper 67-34, Washington, D.C., Jan. 1964.

[23] Fage, A. and Warsap, J. H., "The Effects of Turbulence and Surface Roughness on the Drag of a Circular Cylinder," Aeronautical Research Council, Great Britain, ARC R&M No. 1283, 1930.

[24] Humphreys, J. G., "On a Circular Cylinder in a Steady Wind at Transition Reynolds Numbers," *Journal of Fluid Mechanics*, Vol. 9, Pt. 4, 1960, pp. 603-612.

[25] Schlinker, R. H., Fink, M. R., and Amiet, R. K., "Vortex Noise from Non-Rotating Cylinder and Airfoils," AIAA Paper 76-81, Washington, D. C., Jan. 1976.

[26] Schechenyi, E., "Supercritical Reynolds Number Simulation for Two-Dimensional Flow Over Circular Cylinders," *Journal of Fluid Mechanics*, Vol. 70, Pt. 3, 1975, pp. 529-542.

[27] Ericsson, L. E. and Reding, J. P., "Criterion for Vortex Periodicity in Cylinder Wakes," *AIAA Journal*, Vol. 17, Sept. 1979, pp. 1012-1013.

[28] Kamiya, N., Suzuky, S., and Nishi, T., "On the Aerodynamic Force Acting on a Circular Cylinder in the Critical Range of the Reynolds Number," AIAA Paper 79-1475, Williamsburg, Va., July 1979.

[29] Jacobson, I. D., "Magnus Characteristics of Arbitrary Rotating Bodies," AGARD-AG-171, Nov. 1973.

[30] Kelly, H. R. and van Aken, R. W., "The Magnus Effect at High Reynolds Numbers," *Journal of Aerospace Sciences*, Vol. 23, Nov. 1956, pp. 1053-1054.

[31] Swanson, W. M., "The Magnus Effect: A Summary of Investigations to Date," *Journal of Basic Engineering*, Vol. 83, Sept. 1961, pp. 461-470.

[32] Ericsson, L. E. and Reding, J. P., "Dynamic Stall Analysis in Light of Recent Numerical and Experimental Results," *Journal of Aircraft*, Vol. 13, April 1976, pp. 248-255.

[33] Miller, M. C., "A Technique to Measure the Pressure Distribution on the Surface of Spinning Wind Tunnel Models," *Journal of Aircraft*, Vol. 16, Dec. 1979, pp. 815-822.

[34] Parkinson, G. V. and Ferguson, N., "Amplitude and Surface Pressure Measurements for a Circular Cylinder in Vortex-Excited Oscillation at Subcritical Reynolds Numbers," Paper 18, Meeting on Ground Wind Load Problems in Relation to Launch Vehicles, Langley Research Center, June 1966.

[35] Ferguson, N. and Parkinson, G. V., "Surface and Wake Flow Phenomena of the Vortex-Excited, Oscillation of a Circular Cylinder," *Journal of Engineering for Industry*, Vol. 89, Nov. 1967, pp. 831-838.

[36] Stansby, P. K., "The Locking-On of Vortex Shedding Due to Cross-Stream Vibration of Circular Cylinders in Uniform and Shear Flows," *Journal of Fluid Mechanics*, Vol. 74, Pt. 4, 1976, pp. 641-665.

[37] Koopman, G. H., "The Vortex Wakes of Vibrating Cylinders at Low Reynolds Numbers," *Journal of Fluid Mechanics*, Vol. 28, Pt. 3, 1967, pp. 501-512.

[38] Mei, V. C. and Currie, I. G., "Flow Separation on a Vibrating Circular Clyinder," *The Physics of Fluids*, Vol. 12, Nov. 1969, pp. 2248-2254.

[39] Schindel, L. and Zartarian, G., "Some Water Table Experiments on Oscillating Cylinders," Paper 17, Meeting on Ground Wind Load

Problems in Relation to Launch Vehicles, Langley Research Center, June 1966.

[40] Cincotta, J. C., Jones, G. W., and Walker, R. W., "Experimental Investigation of Wind-Induced Oscillation Effects on Cylinders in Two-Dimensional Flow at High Reynolds Numbers," Paper 20, Meeting on Ground Wind Load Problems in Relation to Launch Vehicles, Langley Research Center, June 1966.

[41] Landl, R., "A Model for Flow-Induced Vibrations," ESROTT-125, Jan. 1975; original report DLR-FB 74-42, 1974.

[42] Hartlen, R. T., Baines, W. D., and Currie, I. G., "Vortex-Excited Oscillations of a Circular Cylinder," Tech. Pub. UTME-TP 6809, University of Toronto, Canada, Nov. 1968.

[43] Ericsson, L. E., "Unsteady Aerodynamics of Separating and Reattaching Flow on Bodies of Revolution," *Recent Research on Unsteady Boundary Layers*, Vol. I, IUTAM Symposium, Laval University, Quebec, Canada, May 1971, pp. 481-512.

[44] Sarpkaya, T., "Vortex-Induced Oscillations—A Selective Review," *Journal of Applied Mechanics*, Vol. 46, No. 2, June 1979, pp. 241-258.

[45] Modi, V. J. and Slater, J. E., "Unsteady Aerodynamics and Vortex Induced Aeroelastic Instability of a Structural Angle Section," AIAA Paper 77-160, Los Angles, Calif., Jan. 1977.

[46] Marris, A. W., "A Review of Vortex Streets, Periodic Wakes, and Induced Vibration Phenomena," *Journal of Basic Engineering*, Vol. 86, June 1964, pp. 185-196.

[47] Tanida, Y., Okajima, A., and Watanabe, Y., "Stability of a Circular Cylinder Oscillating in a Uniform Flow or in a Wake," *Journal of Fluid Mechanics*, Vol. 61, Pt. 4, 1973, pp. 769-784.

[48] Ericsson, L. E. and Reding, J. P., "Vortex-Induced Asymmetric Loads on Slender Vehicles," Lockheed Missiles & Space Company, Inc., Sunnyvale, Calif., Rept. LMSC-D630807, Contract N60921-77C-0234, Jan. 1979.

[49] Hatfield, H. M. and Morkovin, M. V., "Effect of an Oscillating Free Stream on the Unsteady Pressure on a Circular Cylinder," *Journal of Fluids Engineering*, June 1973, pp. 249-254.

[50] Chen, C. F. and Ballengee, D. B., "Vortex Shedding from Circular Cylinders in an Oscillating Freestream," *AIAA Journal*, Vol. 9, Feb. 1971, pp. 340-342.

[51] Durgin, W. W., March, P. A., and Lefebvre, P. J., "Lower Mode Response of Circular Cylinders in Crossflows," *Nonsteady Fluid Dynamics*, ASME Winter Annual Meeting, San Francisco, Dec. 1978, pp. 193-200.

[52] McCroskey, W. J., "The Inviscid Flowfield of an Unsteady Airfoil," *AIAA Journal*, Vol. 11, Aug. 1973, pp. 1130-1137.

[53] McCroskey, W. J., "Recent Developments in Dynamics Stall," *Proceedings of Symposium on Unsteady Aerodynamics*, University of Arizona, Tucson, Arizona, Vol. 1, March 1975, pp. 1-33.

[54] Ericsson, L. E. and Reding, J. P., "Vortex-Induced Asymmetric Loads in 2-D and 3-D Flows," AIAA Paper 80-0181, Pasadena, Calif., Jan. 1980.

[55] Ericsson, L. E. and Reding, J. P., "Quasi-Steady and Transient Dynamic Stall Characteristics," AGARD Symposium on Prediction of Aerodynamic Loading, Moffett Field, Calif., Paper 24, AGARD CP-204, Sept. 1976.

[56] Ericsson, L. E. and Reding, J. P., "Dynamic Stall at High Frequency and Large Amplitude," *Journal of Aircraft*, Vol. 17, March 1980, pp. 136-142

[57] Sarpkaya, T., and Schoaff, R. L., "Inviscid Model of Two-Dimensional Vortex Shedding by a Circular Cylinder," *AIAA Journal*, Vol. 17, Nov. 1979, pp. 1193-1200.

[58] Chapman, D. R., "Dryden Lecture: Computational Aerodynamics Development and Outlook," *AIAA Journal*, Vol. 17, Dec. 1979, pp. 1239-1313.

[59] Ericsson, L. E. and Reding, J. P., "Scaling Problems in Dynamic Tests of Aircraft-Like Configurations," Paper 25, AGARD-CP-227, AGARD Symposium on Unsteady Aerodynamics, Ottawa, Canada, Sept. 1977.